NMR Investigation of a Tetrasaccharide Using Residual Dipolar Couplings in Dilute Liquid Crystalline Media: Effect of the Environment

Clas Landersjö,[†] Christer Höög,[†] Arnold Maliniak,[‡] and Göran Widmalm*,[†]

Department of Organic Chemistry and Division of Physical Chemistry, Arrhenius Laboratory, Stockholm University, S-106 91 Stockholm, Sweden

Received: January 6, 2000; In Final Form: April 4, 2000

The tetrasaccharide lacto-*N*-neotetraose, β-D-Gal*p*-(1→4)-β-D-Glc*p*NAc−(1→3)-β-D-Gal*p*-(1→4)-D-Glc*p*, was investigated by measurements of residual dipolar couplings in two lyotropic liquid crystalline media: (i) prepared from mixtures of dimyristoyl phosphatidylcholine and dihexanoyl phosphatidylcholine in water, and (ii) a ternary system consisting of cetylpyridinium chloride/*n*-hexanol/brine (200 mM NaCl in water). Computer simulations, both Monte Carlo and molecular dynamics, were performed where different force fields were employed. The molecular structures generated were used in the analysis of the experimental dipolar C−H couplings. This analysis indicated that in addition to different orientational tensors, a small conformational difference may be present for the oligosaccharide in the two media. This interpretation emerged from a procedure where the effect of rotation around one central glycosidic torsion angle on dipolar couplings was investigated. Thus, the approach based on measurement of dipolar couplings is a sensitive tool for investigation of molecular conformation.

Introduction

The function of carbohydrates is closely related to their structure with biological responses being dependent on the type and degree of sugar substitution.[1] For oligosaccharides of glycolipids and glycoproteins the conformation that is presented or induced upon interaction with other molecules such as proteins is of specific interest. One way of investigating the role of flexibility and its effect on carbohydrate binding has been by preorganizing the oligosaccharides using intramolecular linkers.[2] The conformation(s) of both the unmodified oligosaccharide and the conformationally restrained molecule are subsequently required to be determined.

The oligosaccharide portion of glycoconjugates has with respect to conformation been investigated in solution by measurements of the ^{1}H,^{1}H nuclear Overhauser effect (NOE), which gives information on distances between proton pairs at the glycosidic linkage.[3] However, too few protons are usually present to adequately describe the possible conformations. The torsion angles for a disaccharide fragment of an oligosaccharide are described by ϕ, at the glycosidic position, and ψ, at the following substituted sugar residue. Long-range *trans*-glycosidic coupling constants related to these torsion angles can be used to obtain additional information on the conformational space available for an oligosaccharide. These carbon-proton couplings, $^3J_{C,H}$, can be obtained experimentally using natural abundance material,[4] while specific ^{13}C labeling of the oligosaccharide is desired to facilitate determination of $^3J_{C,C}$.[5] To provide a relationship between experimentally determined *J* couplings and the molecular structure, it is necessary to invoke a physical model. A frequently used approach is provided by Karplus-type equations that relate the *J* coupling to a torsion angle in the molecule.

Studies of through-space dipole−dipole interactions constitute an extremely powerful tool for molecular structure determination. In anisotropic systems the dipole−dipole couplings can be observed but the resulting proton spectrum even for a medium-sized molecule becomes very complicated. Several techniques, including multiple quantum NMR[6] and deuterium labeling,[7] have been applied in order to simplify the spectra and yet retain the information about the structure and dynamics. At high magnetic fields it has been possible to measure dipolar couplings in solution. These couplings originate from a partial alignment in the static field of the NMR spectrometer due to the magnetic susceptibility of molecules, which facilitates refinement of molecular structure.[8,9] Another method to align molecules, and thus to measure residual dipolar couplings, e.g., ^{1}H,^{13}C and ^{1}H,^{15}N, is to use dilute liquid crystalline solvents.[10] The advantage of these systems is that they enable tuning of the magnitude of the dipolar couplings, since the latter are proportional to the molecular order imposed by the solvent. A few years ago, the formation of bilayerlike assemblies (bicelles) upon mixing of dimyristoyl phosphatidylcholine (DMPC) and dihexanoyl phosphatidylcholine (DHPC) in water was described.[11] These bicelles are particles that have a thickness of ∼40 Å and a diameter of several hundred ångstroms. In a magnetic field the bicelles can, at an appropriate temperature, be ordered to form a dilute liquid crystalline phase, with the normal of the bicelle perpendicular to the magnetic filed. The size of the bicelles (and the degree of ordering) is dependent on the concentration of phospholipids and their ratio q = DMPC/DHPC. Further investigations of this type of mixture including modifications and extensions to obtain larger temperature ranges and more stable preparations together with their applications to biomolecules have been reported recently.[12−25] Other media developed and employed to align molecules for measuring dipolar couplings include a filamentous phage,[26,27] a collodial suspension of rod-shaped viruses,[28] purple membrane fragments,[29,30] or a dilute ternary system containing surfactant/alcohol/brine.[31−33] The general assumption in these studies is that the conformations and dynamics of the nonspherical solute

[†] Department of Organic Chemistry.
[‡] Division of Physical Chemistry.

10.1021/jp000061j CCC: $19.00
Published on Web 05/20/2000

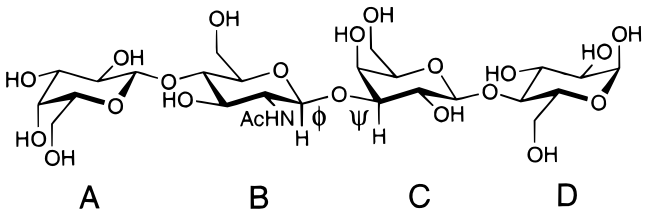

Figure 1. Schematic of the tetrasaccharide lacto-*N*-neotetraose β-D-Gal*p*-(1→4)-β-D-Glc*p*NAc-(1→3)-β-D-Gal*p*-(1→4)-α-D-Glc*p* (LNnT). Torsion angles at glycosidic linkages are denoted by ϕ and ψ. In the text a subscript is used to refer to the pertinent glycosidic linkage. Sugar residues are labeled A through D, starting from the terminal nonreducing end.

molecules addressable by this technique should not be perturbed by the orienting medium per se.

For carbohydrates it was shown that also ^{1}H,^{1}H dipolar couplings can be observed in a DMPC/DHPC aqueous mixture by the application of a DQF−COSY experiment.[34] This should make it possible to describe the relative orientations of sugar rings in an oligosaccharide, even when the residues are spatially apart. The solvent mixture was used to obtain ^{1}H,^{13}C dipolar couplings of the ^{13}C-enriched trisaccharide NeuNAcα2−3Galβ1−4Glc, and these were subsequently used in a dynamical simulated annealing calculation.[35] This led to two families of conformations consistent with experimental data. The same protocol was also used in the study of an oligosaccharide−protein complex.[36] In a recent communication, we investigated the conformation of a tetrasaccharide from human milk lacto-*N*-neotetraose (Figure 1) by measuring residual ^{1}H,^{13}C dipolar couplings in the DMPC/DHPC aqueous mixture.[37] Experimental data were fit to a minimum energy molecular model generated by molecular mechanics. Good agreement was observed for an extended conformation where the linear tetrasaccharide was described as a uniaxial cylinder. However, the agreement was not perfect and no conformational averaging is included in molecular mechanics, which thus prompts further investigation. In the present work we extend the studies of this tetrasaccharide, which has been shown to decrease the incidence of respiratory and ear infections in infants,[38] by further measurements of ^{1}H,^{13}C dipolar couplings in the DMPC/DHPC aqueous mixture and in the dilute ternary system containing cetylpyridinium chloride, *n*-hexanol, and sodium chloride in water. To obtain a consistent picture of the molecular structure, we used Monte Carlo and molecular dynamics simulations for interpretation of the experimental data.

Materials and Methods

Sample Preparation. The tetrasaccharide lacto-*N*-neotetraose[39] (LNnT) β-D-Gal*p*-(1→4)-β-D-Glc*p*NAc-(1→3)-β-D-Gal*p*-(1→4)-D-Glc*p* was obtained from BioCarb Chemicals (Lund, Sweden). The phospholipids, 1,2-dimyristoyl-*sn*-glycero-3-phosphocholine (DMPC) and 1,2-hexanoyl-*sn*-glycero-3-phosphocholine (DHPC) were purchased from Sigma (St. Louis, MO) and Avanti polar lipids (Alabaster, AL), respectively. Cetylpyridinium chloride (CPCl) and sodium chloride (NaCl) were purchased form Merck (Darmstadt, Germany) and *n*-hexanol was obtained from BDH Chemicals (Poole, England), all with a purity >98%. The chemicals were used without further purification.

DMPC and DHPC were carefully weighed and dissolved in D_2O to give two stock solutions containing a total of 8.0% lipid (w/v). After sonication, the solutions were mixed to give a DMPC:DHPC molar ratio of 2.9:1, determined by integration of the peaks in the ^{31}P NMR spectrum. To ensure sample homogeneity, several cycles of cooling (0 °C), sonication, and heating (40 °C) were performed. The CPCl/*n*-hexanol/brine (200 mM NaCl in D_2O) samples were also prepared by weight to give concentrations of 2.0, 3.4, and 5.0% (w/v) with respect to the total content of CPCl/*n*-hexanol, where the two components were added in equal amounts. To the brine/surfactant solution, *n*-hexanol was added and the samples were vortexed. This was followed by equilibration first at 70 °C and then at 30 °C for at least 1 h each. All samples were stored at 4 °C.

The homogeneity of the dilute liquid crystals was checked in the NMR spectrometer by the ^{2}H quadrupolar splitting in D_2O, which was measured as a function of lipid concentration. Sharp lines of equal height are obtained when the sample is homogeneous.[16] When the samples were stable, LNnT (2.0 mg) was dissolved in 600 μL of the liquid crystalline solvent to give a sugar concentration of 4.7 mM.

NMR Spectroscopy. Spectra were acquired using the ^{1}H,^{13}C-gHSQC technique[40,41] on a Varian Inova 600 MHz NMR spectrometer with experimental times of ∼16 h. The digital resolution in the F_2 dimension was 1.2−2.4 Hz, and spectra were zero-filled twice prior to the spectral analysis. For the DMPC/DHPC sample, spectra were obtained at 38 °C (ordered phase) and 25 °C (isotropic phase). Spectra of the three CPCl/*n*-hexanol/brine preparations (ordered phase) and a 200 mM brine solution (isotropic phase) were acquired at 30 °C. The resulting ^{2}H quadrupolar splittings of the CPCl/*n*-hexanol/brine samples were 6.2, 12.8, and 21.1 Hz with increasing concentration of the ternary system. Chemical shifts of LNnT were essentially identical in the two media.

Simulation. Several computer simulations using different force fields were performed. One Metropolis Monte Carlo (MC) simulation was carried out using the GEGOP program[42] (version 2.7) with a force field based on the hard sphere exo-anomeric (HSEA) force field[43] (simulation I). The HSEA force field makes use of rigid carbohydrate residues. The simple potential includes only the ϕ-torsion and van der Waals interactions. A total of 10^6 Monte Carlo steps were performed with an acceptance ratio of 28%. The glycosidic torsion angles were not allowed to move more than 20° in an MC step. Four molecular dynamics (MD) simulations were performed using the molecular mechanics program CHARMM[44] (parallel version, C25b2) with two different force fields, namely CHEAT95[45] (simulation II) and PARM22 (simulations III−V). The CHARMM force field PARM22 (Molecular Simulations Inc., San Diego, CA) is similar to the carbohydrate force field developed by Ha et al.[46] While the two first simulations were performed in vacuo (I and II), the latter three were carried out in aqueous solutions. Initial conditions were created by placing the energy-minimized tetrasaccharide in a previously equilibrated cubic water box of length 40.39 Å containing 2197 TIP3P water molecules and removing those waters that were closer than 2.5 Å to any solute atom. This procedure resulted in a system with the tetrasaccharide and 2132 waters, which was energy minimized using steepest descent, 200 steps, followed by adopted basis Newton−Raphson until the root-mean-square gradient was less than 0.01 kcal mol^{-1} Å^{-1}. MD simulation II with the CHEAT95 force field makes use of extended hydroxyl groups; i.e., hydroxyl hydrogens are absent and the charge of the resulting oxygen is reduced. All MD simulations were started with assignment of initial velocities by different seeds at 100 K, followed by heating with 5 K increments during 8 ps to 300 K, where the systems were equilibrated for 200 ps. The production runs were performed for 2 ns in simulations III−V. Minimum image

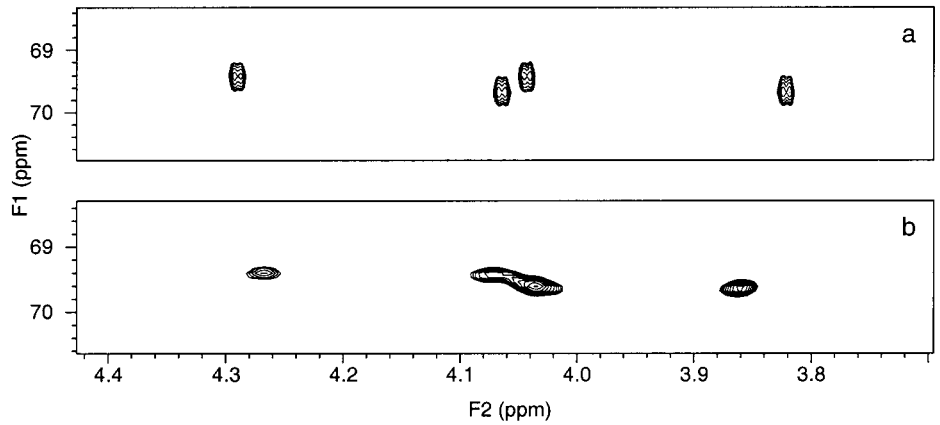

Figure 2. Part of the $^{1}H,^{13}C$ gradient selected HSQC spectrum of LNnT in (a) isotropic brine solution and (b) ordered 5% CPCl/*n*-hexanol/brine solution. The splittings originate from (a) J and (b) $J + D$ and show cross-peaks of A4 (left pair) and C4 (right pair). Note that the D_{CH} are negative for both A4 and C4.

TABLE 1: Dipolar Couplings (Hz) in LNnT (α-Anomeric Form) at 600 MHz in Different Media

sugar residue	atom pair	DMPC/DHPC	CPCl/*n*-hexanol/brine		
		8%	2%	3.4%	5%
A	H4−C4	−19.4	−9.9	−20.2	−39.7
A	H5−C5	16.6	8.1	18.1	37.5
B	H2−C2	22.4	11.8	21.6	40.7
B	H3−C3	24.3	10.9	21.4	37.8
C	H2−C2	19.6	11.7	22.6	41.1
C	H4−C4	−8.4	−7.0	−18.2	−29.9
D	H1−C1	−20.3	−8.2	−19.0	−34.0
D	H5−C5	17.8	10.1	21.8	41.8

boundary conditions were used with a heuristic nonbond frequency update and a force shift cutoff acting to 12 Å. The simulations employed a dielectric constant of unity and a time step of 2 fs, and data were saved every 100 steps for analysis. The SHAKE algorithm was used to restrain hydrogen−heavy atom bonds.[47] The temperature was kept constant using a weak coupling to an external heat bath.[48] The simulation with the CHEAT95 force field spanned 10 ns, without SHAKE restraints, using a time step of 1 fs and a dielectric equal to the distance between the charged particles. The MC simulation was performed on an O_2 workstation (SGI, CA). Simulations II−V were performed on an IBM SP2 computer at the Center for Parallel Computers, KTH, Stockholm. In simulations III−V 32 nodes were used resulting in a CPU time of ∼4 h per 100 ps.

Results and Discussion

I. NMR Measurements. Residual dipolar couplings of the tetrasaccharide LNnT were measured in two different media: (i) DMPC/DHPC bicelles with the phospholipid ratio $q = 2.9$ and concentrations 7.5, 8, and 10% (w/v). The low and high concentrations were in fact used in our previous study.[37] Here we extended these measurements with the intermediate concentration. (ii) The ternary mixture of cetylpyridinium chloride/*n*-hexanol/brine (200 mM NaCl) at concentrations of 2−5%. This system forms a dilute lamellar phase, which can be aligned in the static magnetic field of the NMR spectrometer, with the normal of the bilayer perpendicular to the applied field.

$^{1}H,^{13}C$-gHSQC spectra were acquired to obtain $^{1}J_{C,H}$ couplings in isotropic phases and splittings of the corresponding signals in the liquid crystalline phase, resulting from electron-mediated (J) and through space (D) dipolar couplings present, as shown in Figure 2. The resulting residual C−H dipolar couplings in the ordered phases, given in Table 1, were obtained by subtraction of the $^{1}J_{C,H}$ values determined in the isotropic liquid. All orientationally independent dipolar couplings were determined; both negative and positive couplings were observed. In Figure 3 we show the dependence of the dipolar couplings on the deuterium quadrupolar splitting of D_2O, where the latter reflects the order of the liquid crystalline system. Note that this order is determined by the phospholipid and ternary mixture concentrations for the two media.

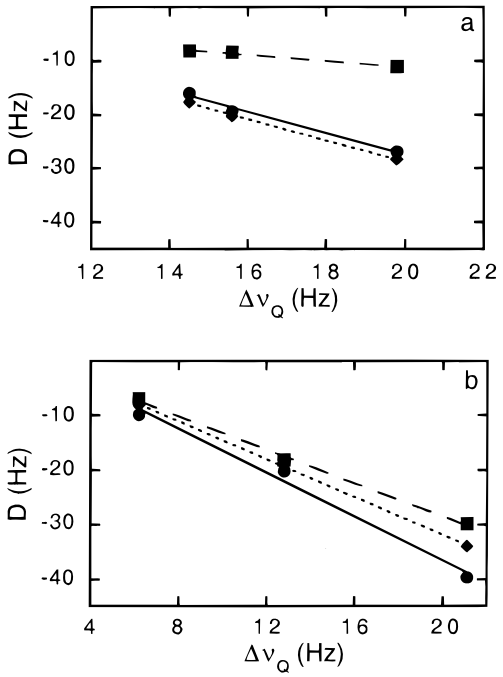

Figure 3. Experimental proton−carbon dipolar couplings of LNnT as a function of the quadrupolar splitting of the D_2O resonance in different media: (a) DMPC/DHPC; (b) CPCl/*n*-hexanol/brine. For clarity only selected C−H pairs are shown: A4 (●), C4 (■), and D1 (◆). Data for 7.5% and 10% DMPC/DHPC solutions are taken from ref 37.

The dipolar couplings with negative values in the bicellar system are shown in Figure 3a. Two of the couplings exhibit similar magnitudes and slopes, while the C4−H4 pair of residue C (denoted C4 in the following discussion) behaves differently. In fact, this coupling showed the largest deviation from the prediction based on the generated molecular model in the previous study.[37] The C−H pairs with positive values of the dipolar coupling were quite similar and so were the slopes (not shown). In Figure 3b the negative dipolar couplings determined in the ternary system are presented. Obviously, the alignment

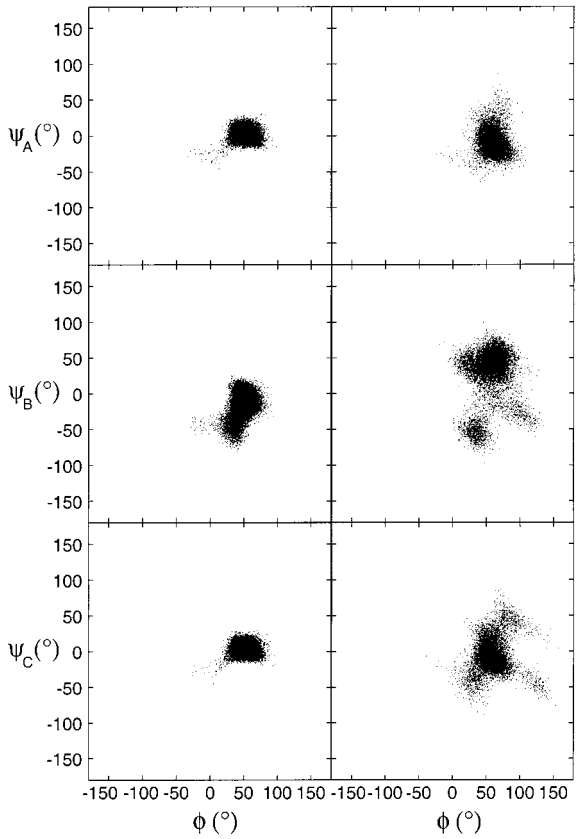

Figure 4. Scatter plots from MC (left column) and MD (right column) simulations of LNnT (simulations I and V, respectively) showing the conformational regions sampled by the three glycosidic linkages in the tetrasaccharide.

range (reflected by the values of D_{CH}) of the LNnT molecule is larger in this phase. The values of the dipolar couplings are quite similar to those observed in the DMPC/DHPC system. However, two important differences may be noted. First, the magnitudes of A4 and D1 have changed compared to the phospholipid preparations. Second, and most importantly, both the slope and the magnitude of C4 have changed dramatically and are here similar to those of A4 and D1. This effect can be explained by a difference in the orientational tensor or of the molecular conformation. Of course, a combination of these two effects is also possible.

II. Molecular Simulations. To perform a quantitative analysis of experimental dipolar couplings, Monte Carlo (MC) and molecular dynamics (MD) simulations of LNnT, using different force fields, were carried out. The results of these computer simulations were used to determine the conformational space available for the molecule. Note that the computations were performed in the isotropic liquid (aqueous solution) and in vacuo, thus assuming that the alignment in the liquid crystalline phases does not significantly affect the molecular structure.

The MC simulation (I) (10^6 steps) was performed in vacuo using the HSEA (hard sphere exo-anomeric) force field. Scatter plots of the glycosidic torsion angles are shown in Figure 4. This force field shows an average of the torsion angle $\psi_B = -16°$, at the central linkage of the oligosaccharide.

MD simulations using the CHEAT95 force field (II) (10 ns) were performed in vacuo, since the force field is derived with united atoms for hydroxyl groups to be simulated without explicit solvent. The flexibility of LNnT obtained from this simulation was substantially larger (not shown). For comparison

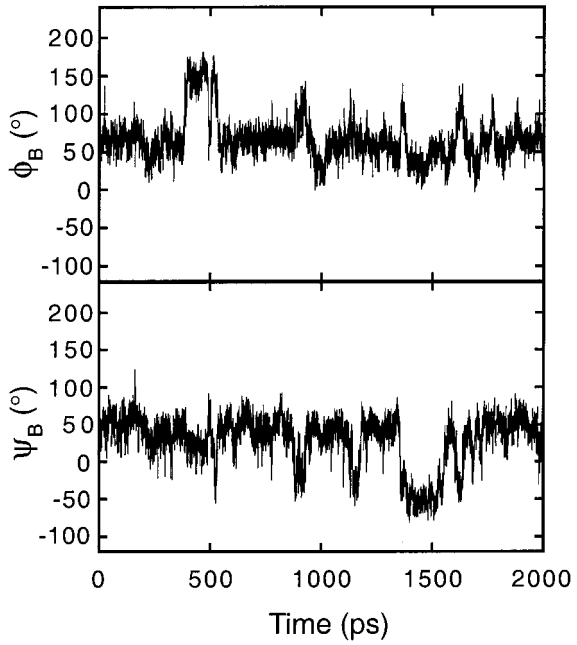

Figure 5. Molecular dynamics trajectories of torsion angles ϕ_B and ψ_B from simulation IV.

the average of the torsion angle $\psi_B = -70°$. Thus, the molecular shape is significantly different in the simulations with these two force fields.

Three MD simulations using the PARM22 force field (III−V) (2 ns each with explicit water present) were performed. In simulation III, a transition occurred early for the torsion angle ϕ_C to an anti-conformer (∼180°), which prevailed for the duration of the simulation. In, simulation IV, transitions to and from anti-ϕ conformations[49] occurred (Figure 5). In both these simulations the molecular shape and therefore the principal axis of the inertial tensor in the molecule is altered compared to all syn states for the glycosidic torsion angles that were sampled in the last simulation (V). In the latter simulation the average of the torsion angle $\psi_B = 29°$. Scatter plots of the glycosidic torsion angles from simulation V are also shown in Figure 4, from which it is evident that the flexibility is larger for the PARM22 force field (right column) compared to HSEA (left column). Thus, the simulations of LNnT describe the conformational space available somewhat differently, with shifts in the averaged values of the glycosidic torsion angles.

III. Data Analysis. The general expression for carbon−proton dipole−dipole couplings is given by[50]

$$D_{CH} = -\frac{\mu_0}{4\pi}\frac{\gamma_C\gamma_H\hbar}{2\pi}\left\langle\frac{1}{2}(3\cos^2\theta - 1)r_{CH}^{-3}\right\rangle \qquad (1)$$

where r_{CH} is the spin−spin distance and θ is the angle between the spin−spin vector and the magnetic field. All other symbols have their usual meaning. To determine the orientation of the C−H vector in a molecular frame, eq 1 is written so as to contain two successive rotations:

$$D_{CH} = -\frac{\mu_0}{4\pi}\frac{\gamma_C\gamma_H\hbar}{2\pi r_{CH}^3}\Big[S_{zz}\frac{1}{2}(3\cos^2\theta_{CH}^z - 1) + (S_{zz} - S_{yy})\frac{1}{2}(\cos^2\theta_{CH}^x - \cos^2\theta_{CH}^y)\Big] \qquad (2)$$

where θ_{CH}^{α} ($\alpha = x, y, z$) are angles between the spin−spin vector and the molecular coordinate frame, here defined by the eigenvectors of the moment of inertia tensor. The order

TABLE 2: Fitting Results for LNnT [Order Parameters ($\times 10^{-3}$)]

		DMPC/DHPC (8%)			CPCl/*n*-hexanol/brine (5%)		
simulation	force field	S_{zz}	$S_{xx} - S_{yy}$	fitting error	S_{zz}	$S_{xx} - S_{yy}$	fitting error
I	HSEA	2.1	0.056	0.38	4.5	0.87	0.20
II	CHEAT95	1.4	−2.4	0.56	2.5	−4.8	0.58
III	PARM22	2.8	1.4	0.50	5.9	2.9	0.36
IV	PARM22	2.5	0.16	0.23	4.8	0.24	0.18
V	PARM22	2.2	−0.12	0.29	4.2	0.042	0.28

parameters, $S_{\alpha\alpha}$, describe the second rotation: namely, the averaged transformation from the molecular axis system to the laboratory space (defined by the magnetic field). Note that, in eq 2, two important assumptions have been introduced: (i) the liquid crystalline phase has a uniaxial symmetry, and (ii) a single ordering matrix is used (indicating a rigid molecule). The presence of internal motion requires additional order parameters.[51] In principle, the expression for every dipolar coupling (eq 2) should be scaled by an appropriate order parameter, *S*, that reflects the flexibility of the spin−spin vector.

In our analysis, eq 2 was numerically fitted to the experimental sets of dipolar couplings. The orientations of the C−H vectors in the molecular coordinate frame, i.e., the angles θ^{α}_{CH}, were determined from the computer simulations by calculating the moment of inertia tensor at every saved time step. Note that these average conformations, generated in the simulation procedures, partly relax the assumption about a rigid molecule, and $\cos^2 \theta^{\alpha}_{CH}$ in eq 2 should be replaced by $\langle \cos^2 \theta^{\alpha}_{CH} \rangle$. Thus, the internal order parameter, *S*, has been implicitly included in eq 2. The C−H distance used in the fitting procedure was 111.7 pm.[52]

The numerical fitting was performed using a program based on the subroutine STEPIT[53] with a procedure that comprised two steps: first a Monte Carlo scan of the parameters followed by a least squares search, to minimize the error square sum. The two adjustable parameters used in the fitting procedure were S_{zz} and $S_{xx} - S_{yy}$. In Table 2 we summarize results of the analysis for two samples representing the different media. The fitting error is defined as

$$N^{-1} \sum_i |D^i_{CH}(\text{exp}) - D^i_{CH}(\text{calc})| / |D^i_{CH}(\text{exp})|$$

where *N* is the number of dipolar couplings. It can be seen that the structure generated using the CHEAT95 force field (simulation II) is not consistent with any of the two sets of experimental dipolar couplings. The fitting errors for both samples are large and the magnitude of the order parameter S_{zz} is smaller than $S_{xx} - S_{yy}$. On the basis of the large fitting errors we do not consider the structures obtained from simulations II and III as reasonable candidates.

From the experiments we know that the sets of dipolar couplings in the two media exhibit significant differences. Thus, at this stage two routes are possible for the analysis of the experimental results: (i) the difference originates from a change in the orientational tensor, or (ii) the LNnT molecule exhibits different conformations in the two liquid crystals. Results in Table 2 indicate that the best agreement (small fitting errors) of the dipolar couplings determined in both samples was obtained using the structure generated in simulation IV. The fitting analysis of simulation IV resulted, however, in an extremely large error of the C4 dipole coupling: the experimental value is −29.9 Hz, while the fitting predicts −2.5 Hz. In fact, this coupling is responsible for almost the entire fitting error, which precludes any further molecular interpretation of this structure. Note that this coupling exhibited the largest sensitivity to the liquid crystalline environment (Figure 3). We conclude, on the basis of the fitting errors, that the two remaining simulations (I and V) are essentially equally good candidates for the description of the real molecule in the two media. The order parameters in Table 2 indicate that the orientational tensors obtained for structures I and V are similar (at least the principal components, i.e., S_{zz}) and sample specific. The general goal of the present analysis is to use the experimental dipolar couplings for investigations of molecular structures. Ideally, therefore, we desire a situation where one of the computer generated structures is consistent with the experiments, while the others clearly deviate.

We will now investigate a possibility of different conformations of LNnT in the two media. An inspection of Figure 4 indicates that the major difference between structures generated in simulations I and V can be ascribed to the torsion angle $\psi_{B,}$ while the distributions of the other torsion angles are similar. In addition, we find that the orientation of the vector corresponding to the C4 dipolar coupling is completely determined by ψ_B. Thus, the proper value of the torsion angle ψ_B, is of crucial importance in the analysis of experimental dipolar couplings. The following section is therefore devoted to investigation of the effect this torsion angle has on various physical parameters, relevant for determination of the molecular structure.

IV. Torsional Rotation. For LNnT, which to a very good approximation can be treated as a cylinder, a rotation at the central glycosidic bond between residues B and C will lead to the largest deviation from this assumption. This part of the molecule would be most prone to a possible conformational change, since for the β-(1→3)-linkage the ϕ-torsion angle is anticipated to be governed by the *exo*-anomeric effect,[54] but close to the ψ-torsion angle an axial secondary hydroxyl group and an equatorial hydrogen are present at C-4 of the galactosyl residue C. It is also at these moieties that the force fields differ in particular. To investigate this, we have performed a torsional rotation of ψ_B, keeping the other glycosidic torsion angles at the average values from simulation V (see Figure 4).

We present in Figure 6 the ψ_B torsional angle dependence of a number of parameters relevant for conformational analyses. There are two classical ways for NMR investigations of molecular structure: (i) torsion angles derived from spin−spin coupling constants such as $^3J_{C,H}$ (Figure 6a) and (ii) determination of proton−proton distances (Figure 6b) by employing NOE measurements. The fitting errors obtained in the analysis of dipolar couplings upon torsional rotation reveal that two regions are consistent with experimental results: around −80° and 0°, where the error values are small (Figure 6c). Calculation of the dipolar coupling as a function of ψ_B for B2 shows that this vector is insensitive to conformational changes (Figure 6d). A much stronger conformational dependence is exhibited by the A4 dipolar coupling (Figure 6e). The orientation of the C4 vector is very sensitive to the torsion angle (Figure 6f), and depending on the conformation, this coupling may alter its sign. In addition, the dipolar couplings need not be interpreted via an empirical function and accurate values are readily obtained.

In Figure 7 we show the difference between the experimental and fitted C4 dipolar coupling derived from the fitting analysis upon rotation of the torsion angle ψ_B for the two media. Two regions of small difference between experimental and calculated couplings are identified, viz., around −100° and 0°. In fact, the former region was found to be highly populated in the simulation with the CHEAT95 force field (simulation II). Thus, based on

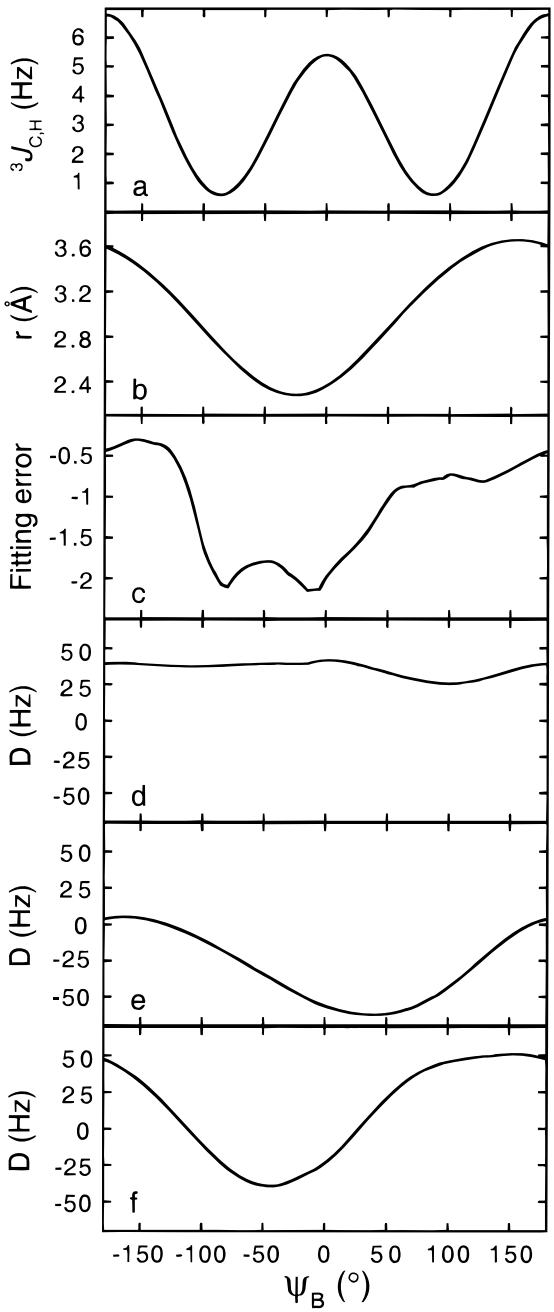

Figure 6. Torsional angle dependence of ψ_B for the β-D-Glc*p*NAc-(1→3)-β-D-Gal*p*-linkage: (a) *trans*-glycosidic $^3J_{C,H}$ value for C-1 in B and H-3 in C; (b) distance between H-1 in B and H-3 in C; (c) fitting error (logarithmic) of the dipolar couplings (see text); (d) B2 dipolar coupling; (e) A4 dipolar coupling; (f) C4 dipolar coupling. All dipolar couplings in comparison to the 8% DMPC/DHPC sample.

the poor agreement with the experimental dipolar couplings (Table 2) we conclude that this region is improbable as the major conformer and the region around 0° is more likely. In the DMPC/DHPC medium the torsion angle in best agreement with experimental data is $\psi_B = 12°$, whereas in the ternary medium a shift to $\psi_B = -5°$ has occurred. Possibly, a change (17°) of the torsion angle has occurred between the two different media, essentially water and brine. This may be illustrated by a molecular overlay of the two conformations based on residues A and B. The difference for residues C and D is then readily seen (Figure 8).

We also tried to prepare a 10% DMPC/DHPC solution with a 200 mM sodium chloride concentration to ascertain the

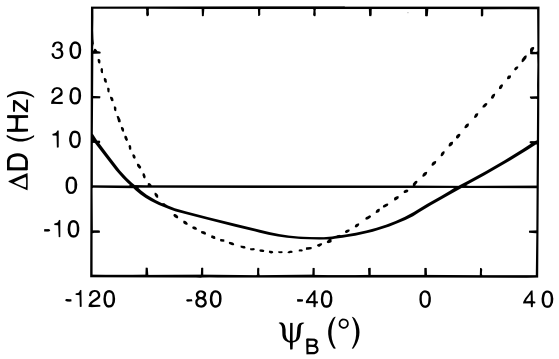

Figure 7. Torsional angle dependence (ψ_B) of the difference between the experimental and calculated C4 dipolar coupling. The curves correspond to different media: 8% DMPC/DHPC (solid); 5% CPCl/*n*-hexanol/brine (dash).

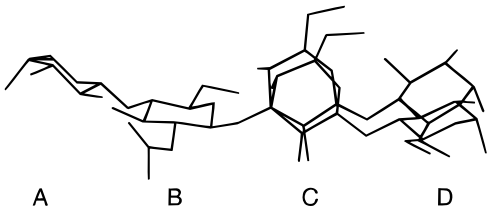

Figure 8. An overlay of LNnT structures, based on residues A and B, representing a possible conformational difference in the two media.

influence of salt in the DMPC/DHPC medium. Recently, a number of phospholipid ratios and concentrations were investigated in the presence of salt.[16] The phase diagrams of these mixtures are complex, and not all combinations are stable. The DMPC/DHPC bicelle preparations do not seem to be able to exist at too high salt concentration, although they exist at lower concentrations used, e.g., when samples are buffered. The bicelles may also be stabilized by the addition of a low amount of cetyltrimethylammonium bromide (CTAB).[55] Initially, an ordered phase was formed in our preparation. However, during the course of the NMR experiment employed in this study a phase separation occurred. The bicelle preparation was not possible to stabilize by the addition of a small amount of CTAB. Thus, at the present time we could not compare the residual dipolar couplings of the DMPC/DHPC preparation in the absence and presence of 200 mM NaCl.

Conclusions

In this paper we have investigated residual dipolar couplings in the tetrasaccharide lacto-*N*-neotetraose dissolved in two lyotropic liquid crystalline media prepared from DMPC/DHPC in water and a ternary system consisting of CPCl/*n*-hexanol/brine. Several dipolar couplings exhibited differences between the two media, and for one particular coupling this effect was dramatic. There are three possible explanations to these differences: (i) a change in the orientational tensor, (ii) a conformational difference, or (iii) a combination of the two. In the absence of a crystal structure for LNnT we performed computer simulations, both Monte Carlo and molecular dynamics, using different force fields. The conformations generated during the simulations were subsequently used in the analysis of the experimental dipolar couplings. Whereas we could reject some of the computational results, different structures were still consistent with the two experimental sets of dipolar couplings. Our analysis indicates that the most realistic description of the systems is provided by case iii, i.e., a change of the orientational tensor combined with a conformational difference. This differ-

ence can, in turn, be attributed to the electrolytic nature of the brine system compared to an essentially aqueous environment in the bicellar solution. However, we cannot rule out the possibility that this conformational difference originates from specific interactions between the LNnT molecule and the aggregates in the liquid crystalline systems (bicelles and bilayers). To identify a single parameter responsible for the molecular conformation in the two media, we performed a systematic rotation of the central torsion angle ψ_B. This procedure resulted in a narrow region that we consider to reflect the conformation of the molecule.

Major tools for determination of molecular structure are based on measurements of spin−spin coupling constants (J) and nuclear Overhauser effects (NOEs), and modifications thereof. For carbohydrates, in particular, trans-glycosidic $^3J_{C,H}$ and $^1H,^1H$ NOEs, are employed to obtain torsion angles and proton distances at the glycosidic linkage. In future work these can be combined with measurement of residual dipolar couplings that provide extremely valuable information about the *orientation* of C−H vectors within the molecule. Thus, the knowledge obtained from these experiments can be employed for further development and assessment of molecular mechanics force field parameters, which in turn can be used with MC and MD simulations to describe conformation, flexibility and dynamics of carbohydrates.

Acknowledgment. This work was supported by grants from the Swedish Natural Science Research Council and Carl Trygger Foundation.

References and Notes

(1) Dwek, R. A. *Chem. Rev.* **1996**, *96*, 683−720.
(2) Bundle, D. R.; Alibés, R.; Nilar, S.; Otter, A.; Warwas, M.; Zhang, P. *J. Am. Chem. Soc.* **1998**, *120*, 5317−5318.
(3) Prestegard, J. H.; Koerner, T. A. W., Jr.; Demou, P. C.; Yu, R. K. *J. Am. Chem. Soc.* **1982**, *104*, 4, 4993−4995.
(4) Rundlöf, T.; Kjellberg, A.; Damberg, C.; Nishida, T.; Widmalm, G. *Magn. Reson. Chem.* **1998**, *35*, 839−847.
(5) Bose, B.; Zhao, S.; Stenutz, R.; Cloran, F.; Bondo, P. B.; Bondo, G.; Hertz, B.; Carmichael, I.; Serianni, S. *J. Am. Chem. Soc.* **1998**, *120*, 11158−11173.
(6) Gamliel, D.; Luz, Z.; Maliniak, A.; Poupko, R.; Vega, A. J. *J. Chem. Phys.* **1990**, *93*, 5379−5386.
(7) Gochin, M.; Schenker, K. V.; Zimmermann, H.; Pines, A. *J. Am. Chem. Soc.* **1986**, *108*, 6813−6814.
(8) Tjandra, N.; Omichinski, J. G.; Gronenborn, A. M.; Clore, G. M.; Bax, A. *Nature Struct. Biol.* **1997**, *4*, 732−738.
(9) Tolman, J. R.; Flanagan, J. M.; Kennedy, M. A.; Prestegard, J. H. *Nature Struct. Biol.* **1997**, *4*, 292−297.
(10) Tjandra, N.; Bax, A. *Science* **1997**, *278*, 1111−1114.
(11) Sanders, C. R.; Schwonek, J. P. *Biochemistry* **1992**, *31*, 8898−8905.
(12) Metz, G.; Howard, K. P.; van Liemt, W. B. S.; Prestegard, J. H.; Lugtenburg, J.; Smith, S. O. *J. Am. Chem. Soc.* **1995**, *117*, 564−565.
(13) Bax, A.; Tjandra, N. *J. Biomol. NMR* **1997**, *10*, 289−292.
(14) Vold, R. R.; Prosser, R. S. *J. Magn. Reson. B* **1996**, *113*, 267−271.
(15) Prosser, R. S.; Hunt, S. A.; DiNatale, J. A.; Vold, R. R. *J. Am. Chem. Soc.* **1996**, *118*, 269−270.
(16) Ottiger, M.; Bax, A. *J. Biomol. NMR* **1998**, *12*, 361−372.
(17) Ramirez, B. E.; Bax, A. *J. Am. Chem. Soc.* **1998**, *120*, 9106−9107.
(18) Prestegard, J. H. *Nature Struct. Biol.* **1998**, *5*, 517−522.
(19) Struppe, J.; Komives, E. A.; Taylor, S. S.; Vold, R. R. *Biochemistry* **1998**, *37*, 15523−15527.
(20) Struppe, J.; Vold, R. R. *J. Magn. Reson.* **1998**, *135*, 541−546.
(21) Losonczi, J. A.; Prestegard, J. H. *Biochemistry* **1998**, *37*, 706−716.
(22) Ottiger, M.; Delaglio, F.; Bax, A. *J. Magn. Reson.* **1998**, *131*, 373−378.
(23) Prosser, R. S.; Volkov, V. B.; Shiyanovskaya, I. V. *Biophys. J.* **1998**, *75*, 2163-2169.
(24) Wang, H.; Eberstadt, M.; Olejniczak, E. T.; Meadows, R. P.; Fesik, S. W. *J. Biomol. NMR* **1998**, *12*, 443−446.
(25) Ottiger, M.; Bax, A. *J. Biomol. NMR* **1999**, *13*, 187−191.
(26) Hansen, M. R.; Mueller, L.; Pardi, A. *Nature Struct. Biol.* **1998**, *5*, 1065−1074.
(27) Hansen, M. R.; Rance, M.; Pardi, A. *J. Am. Chem. Soc.* **1998**, *120*, 11210−11211.
(28) Clore, G. M.; Starich, M. R.; Gronenborn, A. M. *J. Am. Chem. Soc.* **1998**, *120*, 10571−10572.
(29) Koenig, B. W.; Hu, J.-S.; Ottiger, M.; Bose, S.; Hendler, R. W.; Bax, A. *J. Am. Chem. Soc.* **1999**, *121*, 1385−1386.
(30) Sass, J.; Cordier, F.; Hoffmann, A.; Rogowski, M.; Cousin, A.; Omichinski, J. G.; Löwen, H.; Grzesiek, S. *J. Am. Chem. Soc.* **1999**, *121*, 2047−2055.
(31) Prosser, R. S.; Losonczi, J. A.; Shiyanovskaya, I. V. *J. Am. Chem. Soc.* **1998**, *120*, 11010−11011.
(32) Porte, G.; Gomati, R.; El Haitamy, O.; Appell, J.; Marignan, J. *J. Phys. Chem.* **1986**, *90*, 5746−5751.
(33) Gomati, R.; Appell, J.; Bassereau, P.; Marignan, J.; Porte, G. *J. Phys. Chem.* **1987**, *91*, 6203−6210.
(34) Bolon, P. J.; Prestegard, J. H. *J. Am. Chem. Soc.* **1998**, *120*, 9366−9367.
(35) Kiddle, G. R.; Homans, S. W. *FEBS Lett.* **1998**, *436*, 128−130.
(36) Shimizu, H.; Donohue-Rolfe, A.; Homans, S. W. *J. Am. Chem. Soc.* **1999**, *121*, 5815−5816.
(37) Rundlöf, T.; Landersjö, C.; Lycknert, K.; Maliniak, A.; Widmalm, G. *Magn. Reson. Chem.* **1998**, *36*, 773−776.
(38) Kunz, C.; Rudloff, S. *Acta Paediatr.* **1993**, *82*, 903−912.
(39) Kuhn, R.; Gauche, A. *Chem. Ber.* **1962**, *95*, 518−522.
(40) Bodenhausen, G.; Ruben, D. J. *Chem. Phys. Lett.* **1980**, *69*, 185−189.
(41) Willker, W.; Leibfritz, D.; Kerssebaum, R.; Bermel, W. *Magn. Reson. Chem.* **1993**, *33*, 287−292.
(42) Stuike-Prill, R.; Meyer, B. *Eur. J. Biochem.* **1990**, *194*, 903−919.
(43) Thøgersen, H.; Lemieux, R. U.; Bock, K.; Meyer, B. *Can. J. Chem.* **1982**, *60*, 44−57.
(44) Brooks, B. R.; Bruccoleri, R. E.; Olafson, B. D.; States, D. J.; Swaminathan, S.; Karplus, M. *J. Comput. Chem.* **1983**, *4*, 187−217.
(45) Kouwijzer, M. L. C. E.; Grootenhuis, P. D. J. *J. Phys. Chem.* **1995**, *99*, 13426−13436.
(46) Ha, S. N.; Giammona, A.; Field, M.; Brady, J. W. *Carbohydr. Res.* **1988**, *180*, 207−221.
(47) van Gunsteren, W. F.; Berendsen, H. J. C. *Mol. Phys.* **1977**, *34*, 1311−1327.
(48) Berendsen, H. J. C.; Postma, J. P. M.; van Gunsteren, W. F.; DiNola, A.; Haak, J. R. *J. Chem. Phys.* **1984**, *81*, 3684−3690.
(49) Landersjö, C.; Stenutz, R.; Widmalm, G. *J. Am. Chem. Soc.* **1997**, *119*, 8695−8698.
(50) Emsley, J. W. Ed. *Nuclear Magnetic Resonance of Liquid Crystals*; Reidel: Dordrecht, The Netherlands, 1985.
(51) Lipari, G.; Szabo, A. *J. Am. Chem. Soc.* **1982**, *104*, 4546−4559, 4559−4570.
(52) Ottiger, M.; Bax, A. *J. Am. Chem. Soc.* **1998**, *120*, 12334−12341.
(53) Chandler, J. P. Program No. 307; QCPE, Chemistry Department, Indiana University: Bloomington, IN 47405, 1982.
(54) *The Anomeric effect and associated stereoelectronic effects*; Thatcher, G. R. J., Ed.; American Chemical Society: Washington, DC, 1993.
(55) Losonczi, J. A.; Prestegard, J. H. *J. Biomol. NMR* **1998**, *12*, 447−451.